Quantum Late-Time Decay and Channel Dependence

Francesco Giacosa*^{1,2}, Anna Kolbus¹, Krzysztof Kyziol¹, Magdalena Plodowska¹, Milena Piotrowska¹, Karol Szary¹, and Arthur Vereijken¹

¹Jan Kochanowski University, Kielce, Poland ²Goethe University, Frankfurt am Main, Germany

September 23, 2025

Abstract

Quantum mechanics predicts deviations from exponential decay at short and long times, yet experimental evidence is limited. We report a power-law tail after ~ 10 lifetimes in erythrosine B fluorescence, confirmed by two detectors probing distinct bands but yielding different power coefficients. The data match a divergent but normalizable spectral density, and theory predicts oscillations as a future test. A novel and general result is that in multichannel QM (and QFT) decay the lifetime is universal, but the late-time deviations exhibit a sizeable time window in which they are channel- (or band-) dependent, a feature consistent with our data.

Introduction. The exponential law of spontaneous decay, a cornerstone of both non-relativistic quantum mechanics (QM) and relativistic quantum field theory (QFT), is expressed as $P(t) = e^{-t/\tau}$, where P(t) is the survival probability and τ the lifetime of the unstable state. However, this simple law is known to break down at very short and very long times, e.g. [1, 2, 3, 4] for QM and [5, 6, 7] for QFT. At early times, P(t) starts out flat (zero slope, P'(0) = 0), while at later times it turns into a power-law tail [8], $P(t) \sim t^{-(\beta-1)}$, leading to the decay rate intensity $I(t) \propto -P'(t) \sim t^{-\beta}$.

On the experimental side, few confirmations of these deviations exist. At short times, deviations (including both a Zeno and anti-Zeno regimes with slowed and increased decay rates) were measured in tunnelling of sodium atoms through an accelerated optical potential [9, 10]. At long times, deviations were seen in fluorescence decays of various chemical compounds, such as rhodamine and polyfluorene [11]. The decay rate I(t) could be monitored for a very long time with power exponents β ranging between 2–4 and its onset (the 'turnover' time at which the power law starts to dominate) between 8–20 lifetimes.

Besides these measurements, indirect evidence of both short- and long-time deviations was obtained from photons propagating in waveguide arrays [12], where 'time' is replaced by 'space'. In nuclear physics, a late-time power law after 40τ with $\beta=7.4$ in the decay $^8\text{Be} \to \alpha\alpha$ was predicted in Ref. [13] by reconstructing the spectral function from $\alpha\alpha$ scattering data. In the realm of strong interactions, deviations are expected to be large due to large distortions from Breit-Wigner type [14, 15], as confirmed e.g. by the experimental data of Ref. [16]. Anyway, strong decays are too fast for a direct measurement.

In general, for isolated atomic or nuclear systems, the short-time deviations occur extremely early and the long-time ones extremely late, rendering them very hard to observe. A good illustration is the well-known $2P \rightarrow 1S$ transition of the hydrogen atom with $\tau = 1.595\,\mathrm{ns}$. As shown analytically [17] and numerically [18], short-time deviations (both decreased and increased

^{*}corresponding author: fgiacosa@ujk.edu.pl

rate) occur on the attosecond scale¹ $(10^{-9}\tau)$, while late-time deviations start at $200 \,\mathrm{ns}$ (125τ) , when basically no excited atoms remain. These facts explain why deviations could be observed in engineered optical potentials at short times, or in dye fluorescence with very good precision at late times. Since the work of Rothe *et al.* [11], however, (to our knowledge) no independent confirmation in other systems has been reported.

Aim. The aim of the present work is to investigate, both experimentally and theoretically, the late-time decay. Molecules decaying via fluorescence provide an optimal environment for verifying late-time deviations. To this end, we investigate the fluorescence decay in organic dyes, among which one of them (erythrosine B) exhibits clear deviations from the exponential behaviour at late times. A novelty of our late-time study is the use of two detectors operating in distinct spectral windows. While both channels report the same exponential lifetime, the coefficients of the late-time power law differ, with $\beta \approx 1.5$ and $\beta \approx 2.0$ respectively, see details below.

This observation compelled us to examine the quantum decay law at large times in greater generality. Remarkably, the measured values of the power–law exponent β can only arise from very specific forms of the spectral function. Even more significantly, the analysis forced us to reconsider the properties of the multichannel decay law at late times [6, 7], showing that quantum mechanics indeed allows for distinct power laws to emerge in different spectral bands. In this context we also establish novel general relations, which are not restricted to a specific system but should hold for any unstable quantum state.

Experiment: setup and results. The experiment was performed on a Nikon Eclipse Ti-E inverted confocal microscope equipped with two picosecond laser diodes as an excitation source (PicoQuant LDH-D-C-440 with wavelength 438 nm and PicoQuant LDH-D-C-485 with wavelength 483 nm – pulse widths < 120 ps, spectral widths ranging from 2 to 8 nm; only the former was used). Fluorescence from the sample was coupled via optical fibres into a dual-channel detection unit (PicoQuant PMA Hybrid 40 photomultipliers, timing resolution <120 ps), separated by a dichroic mirror and bandpass filters (520/35 nm and 600/50 nm). Time-correlated single-photon counting was carried out with a PicoHarp 300 module. This dual-detector scheme allowed us to record fluorescence decay simultaneously in two distinct spectral windows. The four dyes (fluorescein, acridine orange, rhodamine B, erythrosine B) were dissolved in methanol with a solution concentration of 10⁻⁵ mol/dm³. While fluorescein, acridine orange, and rhodamine B can be described by a single or two-exponential function (plus background), erythrosine B exhibited a clear non-exponential behaviour at late times. Hence, below we concentrate on erythrosine B. In total, seven fluorescence decay curves were obtained (three measurements (10 min each) in October 2024, two in November 2024, and two in February 2025, 15 min each). These data sets were combined together and are reported in Fig. 1. Also the IRF (Instrument Response Function) was measured. Subsequently, the convolution of the signal was performed, but the influence of the IRF turned out to be negligible for our late-time study.

We used two different fitting models presented in Table 1: a two-exponential function and an exponential one plus a power law. The fit results are reported in Table 2: the non-exponential model describes the data significantly better than the two-exponential one. This is confirmed in Fig. 1, where the exponential fit first systematically underestimates data (up to 5 ns), and then systematically overshoots them (between 5 and 15 ns), and so on.

Interpretation/1: shape of the spectral function. Turning to the interpretation of the data, we need to assess to what extent QM accounts for the observations². In QM, deviations from the exponential law can be understood by studying the survival amplitude

$$\mathcal{A}(t) = \int_{E_{th}}^{\infty} dE \, \rho(E) \, e^{-iEt/\hbar},\tag{1}$$

¹This region could be tested by using short attosecond laser pulses, e.g. [19].

²Delayed fluorescence occurs on much longer timescales and presumably cannot explain our data [20]. Non-exponential fluorescence has also been reported in ensembles of distinct states as well as through singlet–triplet population recycling [21]; for a broader overview of these and other molecular processes distorting the decay rate, see Ref. [22].

Table 1: Model functions employed in the analysis; $t \gtrsim 2t_0$ and b is the background. Note, t_0 is not part of the fit parameter, but is taken as the maximum of the intensity.

Model	Fluorescence intensity $I(t)$	Fit parameters
Two-exponential	$I(t) = C_1 \exp\left(-\frac{t-t_0}{\tau_1}\right) + C_2 \exp\left(-\frac{t-t_0}{\tau_2}\right) + b$	$\chi^2(C_1, \tau_1, C_2, \tau_2, b)$
Nonexponential	$I(t) = C \exp\left(-\frac{t-t_0}{\tau}\right) + C_p (t-t_0)^{-\beta} + b$	$\chi^2(C_0, \tau, C_p, \beta, b)$

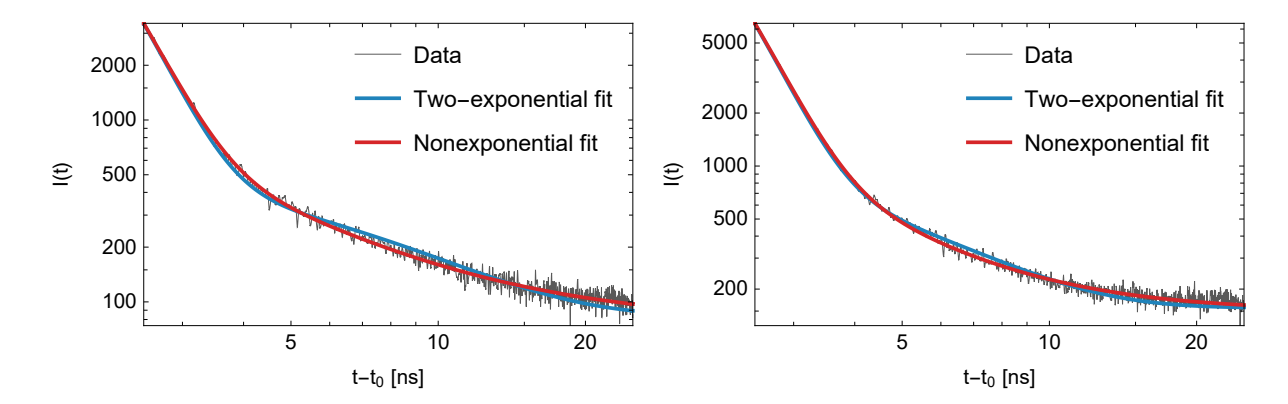


Figure 1: Fluorescence Intensity for both photon detectors (channel 1: left, channel 2: right) - comparison between data and both fitting functions up to ~ 20 ns (data taking up to ~ 95 ns).

Table 2: Fitting results for Erythrosine B measurements.

Fitting Range - Channel 1: 0.960 - 94.752 ns; Channel 2: 0.960 - 94.656 ns;								
Two-exponential model								
Channel	$\chi^2_{ u}$	C_1	$ au_1 \; [ext{ns}]$	C_2	$\tau_2 [\mathrm{ns}]$	b		
1	1.219	665 627	0.46105	574.44	5.3898	83.80		
2	1.256	1 353 960	0.45583	1 348.40	3.40912	156.53		
Nonexponential model								
Channel	$\chi^2_{ u}$	C	$\tau \text{ [ns]}$	C_p	$\beta \text{ [ns]}$	b		
1	1.049	692 886	0.44802	2 929.81	1.5469	77.03		
2	1.080	1 357 800	0.4475	7 687.33	1.9985	150.01		

where $\rho(E)$ is the energy distribution of the unstable quantum state and E_{th} its minimal energy³. The survival probability $P(t) = |\mathcal{A}(t)|^2$ satisfies P(0) = 1, in turn implying $\int_{E_{th}}^{\infty} dE \, \rho(E) = 1$. For a Breit-Wigner distribution with $E_{th} \to -\infty$ and $\rho(E) = \frac{\Gamma}{2\pi} ((E - M)^2 + \Gamma^2/4)^{-1}$, the exponential law $P(t) = e^{-\Gamma t}$ emerges. For realistic systems, $\rho(E)$ falls off faster than E^{-2} , implying P'(0) = 0. The presence of a finite threshold E_{th} is responsible for the long-time power law.

Th late-time behaviour can be modelled by an energy-dependent width $\Gamma \to \Gamma(E)$ with near-threshold scaling $\Gamma(E) \sim (E - E_{th})^{\gamma}$ [1]. (For instance, in QFT decays $\gamma = (2L+1)/2$ with L the relative angular momentum, e.g. [23].) For transparency, we adopt the following simple

³In QFT one has similar features upon substituting $E \to s = E^2$, leading to $\mathcal{A}(t) = \int_{s_{th}}^{\infty} ds \, \rho(s) \, e^{-i\sqrt{s}t/\hbar}$.

model:

$$\rho(E) = \mathcal{N} \frac{E^{\gamma}}{(E - E_0)^2 + \Gamma^2/4} \,\theta(E),\tag{2}$$

where \mathcal{N} normalizes $\mathcal{A}(0) = 1$, $\tau = \hbar/\Gamma$, and $E_0 = M - E_{th}$. Here, the energy dependence is retained only in the numerator, while $\Gamma \approx \Gamma(E_0)$ is used in the denominator⁴. The exponent γ determines the late-time scaling: $A(t) \sim t^{-(\gamma+1)}$, hence $P(t) \sim t^{-2(\gamma+1)}$ and $I(t) \sim t^{-(2\gamma+3)} = t^{-\beta}$ (thus, $\beta = 2\gamma + 3$). The offset E_0 controls the turnover time: the smaller E_0 , the earlier the power-law sets in. Normalizability demands $\gamma > -1$; for $-1 < \gamma < 0$ the spectral function diverges at threshold but remains integrable, leading to $1 < \beta < 3$. Our measured value(s) of β lie precisely in this range. Thus, quantum effects can explain the measured power law, provided that the density near threshold behaves as $\rho(E) \propto E^{\gamma<0}$. For channel 1, the appropriate spectral function and the survival probability are shown in Fig. 2. Interestingly, P(t) also shows pronounced oscillations due to the distorted threshold⁵. In the physical case, these oscillations are washed out by ensemble averaging and the finite time-binning of detection, but they remain an intriguing prediction for future high-resolution studies (assuming, of course, that the QM explanation applies).

It is interesting to note that values of $1 < \beta < 3$ (for which $\gamma < 0$) are also listed in Ref. [11]. (Other interpretations of these results, in terms of spectral filtering effects [24] or sample disorder [25], have also been discussed.) Thus, a similar shape of the spectral function as in Fig. 1, left panel, would also be required to describe the results in [11]. It remains an open question which physical mechanisms—whether related to the laser pulse generation or to internal molecular interactions—could be responsible for such a shape. If it originates from the state formation process, then altering the preparation conditions should modify the result, a possibility that is experimentally testable.

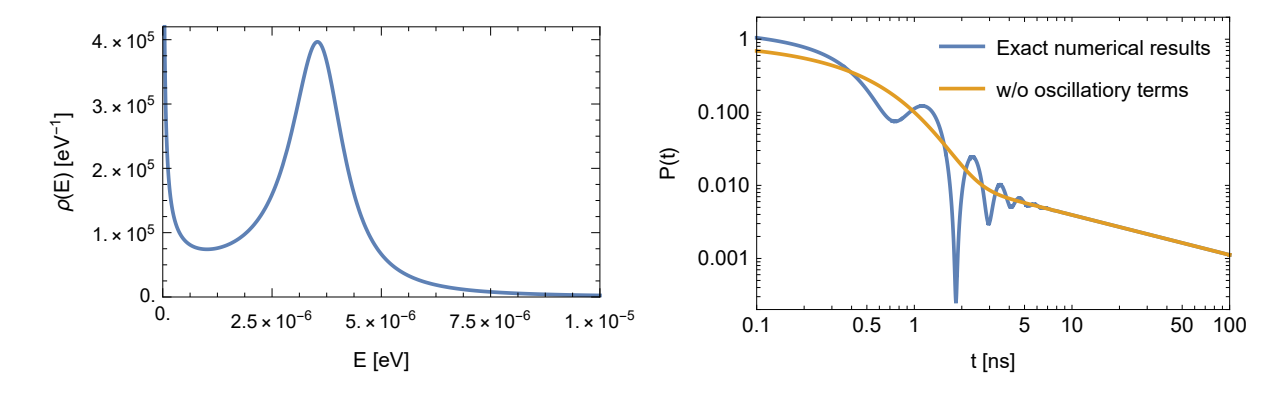


Figure 2: Spectral function $\rho(E)$ (left) and the corresponding survival probability (right), where oscillations appear (the superimposed curve is the coarse-grained outcome without oscillations $(t \gtrsim 2t_0)$). The numerical values are chosen to reproduce the turnover and the late-time power law of channel 1 of Fig. 1.

Interpretation/2: multichannel decay at late times. The two detectors measure the same exponential lifetime τ but different power law coefficients, see Table 2. Now, for the QM interpretation to be attainable, it should, at least qualitatively, explain this feature. To this end, we first note that in molecular fluorescence, the relevant electronic states are S_0 (ground singlet state) and S_1 (first excited singlet state) [26]. After absorption and rapid vibrational relaxation, the molecule resides in the lowest vibrational level of S_1 . This is a "narrow" initial state. Fluorescence corresponds to the radiative transition $S_1 \to S_0$, but the final state is not unique: the electron may decay into any of the many vibrational sublevels of S_0 . Each such

 $^{^4}$ In general, the mass/energy correction becomes energy dependent, see [6, 15] and refs. therein for details.

⁵Note, while the presence of oscillations is general, the specific amplitude depends on the employed model.

transition emits a photon with energy $E_{\gamma} = E(S_1, v = 0) - E(S_0, v_i)$, where i labels a level in S_0 [27, 28]. The relative intensity at each photon energy is given by the overlap of wave functions (the emission being stronger for larger overlaps). The total decay width of the excited state is the sum of the partial widths into all available channels, $\Gamma_{\text{tot}} = \sum_i \Gamma_i$, with each Γ_i corresponding to decay into one specific level. In the case of exponential decay, the intensity of a given decay channel is given by $I_i(t) \propto (\Gamma_i/\Gamma)e^{-\Gamma t}$, see e.g. [7, 29]. Then, no band/channel difference takes place.

Yet, the picture changes when non-exponential deviations are accounted for. The theory for multichannel decay was derived by one of us (F. G.) [6, 7]. In order to keep the discussion as simple as possible, let us consider only two channels. For the fluorescence system, they 'roughly' represent the two detector bands (clearly, this is a simplification since each band contains multiple channels, but the main outcome can be generalized to more realistic cases). The total spectral function is the sum of two channels, $\rho(E) = \rho_1(E) + \rho_2(E)$, with

$$\rho_i(E) = \mathcal{N} \frac{c_i (E - E_{th,i})^{\gamma_i}}{(E - M)^2 + \Gamma^2 / 4} . \tag{3}$$

The probability that the decay takes place in the i-th channel between the time interval (0, t > 0)reads [6]:

$$w_i(t) = \int_{E_{th,i}}^{\infty} dE \frac{\Gamma_i(E)}{2\pi} \left| \int_0^t \mathcal{A}(t') e^{iEt'/\hbar} dt' \right|^2, \, \Gamma_i(E) = c_i \left(E - E_{th,i} \right)^{\gamma_i}. \tag{4}$$

For sufficiently large t, when the power-law domain sets in and for a large time interval, $w_i(t)$ can be approximated by⁶:

$$w_i(t) = w_i(\infty) - a_i t^{-(\gamma_1 + \gamma_2 + 2)} - b_i t^{-2(\gamma_i + 1)} - \dots,$$
(5)

where $w_i(\infty) = \int_{E_{th}}^{\infty} dE \rho_i(E) \approx \Gamma_i/\Gamma$ is the branching ratio for the *i*-channel, and a_i and b_i are appropriate coefficients⁷. For definiteness, let us consider $\gamma_1 < \gamma_2$. Then, the distinct channel intensities read:

$$I_1(t) \propto w_1'(t) \propto t^{-2\gamma_1 + 3} ; I_2(t) \propto w_2'(t) \propto t^{-(\gamma_1 + \gamma_2 + 3)} .$$
 (6)

This is a quite remarkable property: the late-time behaviour is at the onset of the non-exponential behaviour channel-dependent. This feature is general and can be applied to any QM or QFT decay at late times, provided that at least two channels are present. The powers depend solely on the behaviour of the partial spectral functions at thresholds (the parameters γ_i), hence the turnover times may also differ.

Extending the discussion to N channels, the qualitative picture is quite simple: there is a dominating amplitude $\mathcal{A}(t) \propto t^{-(\gamma_{\min}+1)}$ (leading to the overall decay intensity $I(t) \propto t^{-(2\gamma_{\min}+3)}$), where γ_{\min} is the overall minimal γ . As such, it enters in all channels, but the channel-dependent intensity $I_i(t)$ scales as $t^{-(\gamma_{\min}+\gamma_i+3)}$. If a certain band is taken into account, the behaviour of the band is

$$I_{band}(t) \propto \sum_{i=1}^{N_{band}} \left(a_i t^{-(\gamma_{\min} + \gamma_i + 3)} + b_i t^{-(2\gamma_i + 3)} \right) \propto t^{-(\gamma_{\min} + \gamma_{B,\min} + 3)} , \qquad (7)$$

where γ_{\min} does not need to belong to the band, and $\gamma_{B,\min}$ is the minimal value within the band (for $\gamma_{B,\min} = \gamma_{\min}$, $I_{band}(t) \sim I(t) \sim t^{-(2\gamma_{\min}+3)}$).

⁶Using $\int_0^t \mathcal{A}(t')e^{iEt'/\hbar}dt' = \mathcal{G}(E) - \int_t^\infty \mathcal{A}(t')e^{iEt'/\hbar}dt'$ where $\mathcal{G}(E)$ is the propagator, the scaling of Eq. (6)

appears when the modulus squared is approximated as: $|...|^2 \approx |\mathcal{G}(E)|^2 - \mathcal{G}^*(E) \int_t^\infty \mathcal{A}(t') e^{iEt'/\hbar} dt' - h.c.$.

The restingly, Eq. (6) can be also obtained by using the approximate expressions of Ref. [7]: $w_i(t) = w_i(\infty) - \text{Re}[\mathcal{A}(t)\mathcal{A}_i^*(t)]$ with $\mathcal{A}_i(t) = \int_{E_{th,i}}^\infty dE \rho_i(E) E^{-iEt/\hbar}$.

The feature above may explain the different power laws for the different detectors, see Fig. 1 and Table 2. The fact that the two detectors have (a small) overlap does not affect the picture, as long as the minimal values of $\gamma's$ do not coincide. Namely, $I_{band}^{(1)}(t) \sim t^{-(\gamma_{\min}+\gamma_{B_1,\min}+3)}$ and $I_{band}^{(2)} \sim t^{-(\gamma_{\min}+\gamma_{B_2,\min}+3)}$ are, in general, distinct. The inclusion of different thresholds, the transition to a continuous model, and the onset of power tails is left as an outlook. They, however, do not change the main result that the power law is for a long-time channel (or band) dependent.

Concluding remarks. In this work, we have shown that the fluorescence decay of erythrosine B is well described by power law curves (Fig. 1). For this to be a QM non-exponential decay as in Ref. [1], the spectral function must have a peculiar behaviour close to the left-threshold to reproduce the measured intensity (Fig. 2). Moreover, based on Ref. [6] and extending it, we have shown a general feature of multichannel quantum decays (of any type, thus valid in principle for any quantum unstable state, from elementary particles to molecular compounds): contrary to the exponential decay with $\Gamma = \tau^{-1}$ common to any decay channel, the coefficient of the power law depends on the specific channel (or, more generally, the band). Roughly speaking, since the power-law tail reflects a memory that the quantum system retains of its creation time, this memory is channel-dependent, and therefore 'frequency' (or 'colour') dependent. This property is consistent with the different power law coefficients that we measured.

Future work on late-time multichannel decay is needed, both theoretically and experimentally, due to the complex nature of the system. Besides fluorescence, late-time deviations could also be investigated in the context of quantum tunnelling [4, 30], as e.g. the asymmetric potential well with two decay channels (left/right) of Ref. [31]. Applications to other systems, such as nuclear decays or even elementary particles, may also offer valuable opportunities to test these quantum predictions.

Acknowledgments We thank M. Gaździcki, M. Pajek, P. Moskal, M. Skurzok, G. Pagliara, and S. Sharma for useful discussions. We also thank the Institute of Biology of the Jan Kochanowski University, in particular the head of the medical biology department, M. Arabski, for access to the facility. This work was supported by the Minister of Science (Poland) under the 'Regional Excellence Initiative' program (projects no. RID/SP/0015/2024/01 and no. RID/2025/LIDER/02).

References

- [1] L. Fonda, G.C. Ghirardi, and A. Rimini. Decay theory of unstable quantum states. *Rep. Prog. Phys.*, 41:587–631, 1978.
- [2] P. Facchi and S. Pascazio. Quantum Zeno dynamics: mathematical and physical aspects. *J. Phys. A*, 41(49):493001, 2008.
- [3] A. G. Kofman and G. Kurizki. Acceleration of quantum decay processes by frequent observations. *Nature*, 405(6786):546–550, 2000.
- [4] Duane A. Dicus, Wayne W. Repko, Roy F. Schwitters, and Todd M. Tinsley. Time development of a quasistationary state. *Phys. Rev. A*, 65(3):032116, 2002.
- [5] P. Facchi and S. Pascazio. Van Hove's ' $\lambda^2 t$ ' limit in nonrelativistic and relativistic field theoretical models. *Chaos Solitons Fractals*, 12:2777, 2001.
- [6] Francesco Giacosa. Multichannel decay law. Phys. Lett. B, 831:137200, 2022.
- [7] Francesco Giacosa. Non-exponential decay in quantum field theory and in quantum mechanics: the case of two (or more) decay channels. *Found. Phys.*, 42:1262–1299, 2012.

- [8] L. A. Khalfin. On the theory of the decay at quasi-stationary state. *Doklady Akad. Nauk S.S.S.R.*, Vol: 115, 07 1957.
- [9] S.R. Wilkinson, C.F. Bharucha, M.C. Fischer, K.W. Madison, P.R. Morrow, Q. Niu, B. Sundaram, and M.G. Raizen. Experimental evidence for non-exponential decay in quantum tunnelling. *Nature*, 387(6633):575–577, 1997.
- [10] M. C. Fischer, B. Gutiérrez-Medina, and M. G. Raizen. Observation of the quantum zeno and anti-zeno effects in an unstable system. *Phys. Rev. Lett.*, 87:040402, 2001.
- [11] C. Rothe, S. I. Hintschich, and A. P. Monkman. Violation of the Exponential-Decay Law at Long Times. *Phys. Rev. Lett.*, 96(16):163601, 2006.
- [12] A. Crespi, F.V. Pepe, P. Facchi, F. Sciarrino, P. Mataloni, H. Nakazato, S. Pascazio, and R. Osellame. Experimental investigation of quantum decay at short, intermediate, and long times via integrated photonics. *Phys. Rev. Lett.*, 122:130401, 2019.
- [13] N. G. Kelkar, M. Nowakowski, and K. P. Khemchandani. Hidden evidence of nonexponential nuclear decay. Phys. Rev. C, 70:024601, 2004.
- [14] Francesco Giacosa and Giuseppe Pagliara. On the spectral functions of scalar mesons. *Phys. Rev. C*, 76:065204, 2007.
- [15] F. Giacosa, A. Okopińska, and V. Shastry. A simple alternative to the relativistic Breit–Wigner distribution. *Eur. Phys. J. A*, 57(12):336, 2021.
- [16] S. Schael et al. Branching ratios and spectral functions of tau decays: Final ALEPH measurements and physics implications. *Phys. Rept.*, 421:191–284, 2005.
- [17] P. Facchi and S. Pascazio. Temporal behavior and quantum zeno time of an excited state of the hydrogen atom. *Phys. Lett. A*, 241:139–144, 1998.
- [18] F. Giacosa and K. Kyzioł. Nonexponential Decay Law of the 2P–1S Transition of the H Atom. Acta Phys. Polon. A, 146(5):704–708, 2024.
- [19] André D. Bandrauk, Jing Guo, and Kai-Jun Yuan. Circularly polarized attosecond pulse generation and applications to ultrafast magnetism. *J. Opt.*, 19(12):124016, 2017.
- [20] Gauthier Croizat, Aurélien Gregor, Emmanuel Gerelli, Jaroslava Joniova, Marek Scholz, and Georges Wagnières. A general framework for non-exponential delayed fluorescence and phosphorescence decay analysis, illustrated on protoporphyrin ix. *Journal of Photochemistry and Photobiology B: Biology*, 209:111887, August 2020. Provided by the SAO/NASA Astrophysics Data System.
- [21] J. Wlodarczyk and B. Kierdaszuk. On the origin of non-exponential fluorescence decays in enzyme-ligand complex. *Proc SPIE*, 5330, 05 2004.
- [22] É. S. Medvedev. Nonexponential fluorescence decay of polyatomic molecules. *Soviet Physics Uspekhi*, 34(1):16–35, January 1991.
- [23] Claude Amsler and Frank E. Close. Is f0 (1500) a scalar glueball? Phys. Rev. D, 53:295–311, 1996.
- [24] J. Martorell, J. G. Muga, and D. W. L. Sprung. Long time deviation from exponential decay: non-integral power laws. *Phys. Rev. A*, 75:012702, 2007.
- [25] R. Carminati, L. S. Froufe-Pérez, and J. J. Sáenz. Fluorescence lifetime statistics of molecules in disordered media. *Phys. Rev. Lett.*, 99:123903, 2007.

- [26] J. Lakowicz. *Principles of Fluorescence Spectroscopy, 3rd Edition*, volume 1. Springer, 01 2006.
- [27] Xiujuan Zhuang, Anh Le, Timothy C. Steimle, N. E. Bulleid, I. J. Smallman, R. J. Hendricks, S. M. Skoff, J. J. Hudson, B. E. Sauer, E. A. Hinds, and M. R. Tarbutt. Franck–condon factors and radiative lifetime of the $a^2\pi_{1/2}$ – $x^2\sigma^+$ transition of ytterbium monofluoride, ybf. *Phys. Chem. Chem. Phys.*, 13(42):19013–19024, 2011.
- [28] A. Manian, R. A. Shaw, I. Lyskov, W. Wong, and S. P. Russo. Modeling radiative and non-radiative pathways at both the franck—condon and herzberg—teller approximation level. J. Chem. Phys., 155(5):054108, 2021.
- [29] Rafael de la Madrid. The decay widths, the decay constants, and the branching fractions of a resonant state. *Nucl. Phys. A*, 940:297–310, 2015.
- [30] Murray Peshkin, Alexander Volya, and Vladimir Zelevinsky. Non-exponential and oscillatory decays in quantum mechanics. *EPL*, 107(4):40001, 2014.
- [31] Francesco Giacosa, Przemysław Kościk, and Tomasz Sowiński. Capturing nonexponential dynamics in the presence of two decay channels. *Phys. Rev. A*, 102(2):022204, 2020.